PN-AAL-212

BOT. GAZ. 143(1):41-51. 1982.
© 1982 by The University of Chicago. All rights reserved.
0006-8071/82/4301-0006$02.00

MORPHOGENESIS OF EFFECTIVE AND INEFFECTIVE ROOT NODULES IN PHASEOLUS VULGARIS L.

LISA MORRISON BAIRD AND BARBARA D. WEBSTER

Department of Agronomy and Range Science, University of California, Davis, California 95616

Seedlings of *Phaseolus vulgaris*, inoculated with an effective strain of *Rhizobium phaseoli* (CIAT 73) or an ineffective strain (14c), were maintained on an N-free nutrient solution in sterilized sand. Acetylene reduction was measured periodically, and nodules were harvested for light and electron microscopy. In plant host cells infected with CIAT 73, there was an increase in cell volume, nuclear size, and mitochondrial length as bacteria multiplied and became bacteroidal. Golgi activity and rough endoplasmic reticulum (RER) were sparse at nodule maturity, but close associations of amyloplasts and elongated, energized mitochondria were observed. Nitrogen fixation peaked at 5 wk and dropped sharply coincident with flowering. Plant host cells infected with 14c typically contained numerous mitochondria; Golgi bodies and RER were conspicuous throughout nodule development. By the time the bacteria became bacteroidal, plant shoots were chlorotic, and under nitrogen stress the apex had made the transition to flowering. Data suggest that such ineffective nodulation may accelerate the process of normal nodule senescence.

Introduction

For nearly a century it has been known that strains of *Rhizobium* vary in ability to nodulate and benefit a legume host. Ineffective root nodules that do not fix molecular nitrogen may be the result of environmental factors or mutations in the host or bacterial genome. Such nodules reportedly differ physiologically and/or anatomically from effective nodules on the same species (HOLL 1973; PANKHURST 1974; BERGERSEN 1974, NEWCOMB, SYŌNO, and TORREY 1977).

Studies of ineffective nodulation suggest that establishment of an effective legume–*Rhizobium* association can fail at any one of several stages. BERGERSEN (1957), e.g., described an association in which bacteria were not released from the infection thread. However, if infection occurs, the symbiosis usually breaks down either sometime after bacterial release from the thread and prior to transformation to the bacteroidal form, or immediately following transition to the bacteroidal form (CHEN and THORNTON 1940; MACKENZIE and JORDAN 1974; BASSETT, GOODMAN, and NOVACKY 1977*a*, 1977*b*).

Early research on nodulation in *Phaseolus vulgaris* L., the common bean, indicated that all plant/rhizobial interactions were ineffective (FRANK 1890; SCHNEIDER 1892; DAWSON 1900). On the basis of cytological and histological data, MCCOY (1929) suggested that ineffectiveness was ultimately caused by bacterial malnutrition as a result of large amounts of starch stored in the nodule cortex. This starch was supposedly unavailable to the bacteria and thus limited their transformation into bacteroids. Effective nodulation in *P. vulgaris* was reported by WILSON and LELAND (1929) and SEARS and CLARK (1930), but subsequent research indicated that most strains of *Rhizobium phaseoli* were of little benefit to the plant (FRED, BALDWIN, and MCCOY 1932; GRAHAM and HALLIDAY 1977).

Few attempts have been made to examine effective and ineffective nodulation in *P. vulgaris* (LIMA NOGUEIRA, MARTINS DA SILVA, and SAITO 1979), and there are no comprehensive studies relating ultrastructural changes during nodule morphogenesis to whole plant development.

This research was undertaken to compare the ultrastructural characteristics and nodule and plant morphogenesis in effectively and ineffectively nodulated plants of *P. vulgaris*.

Material and methods

Seeds of *Phaseolus vulgaris* L. 'Red Kidney' were surface sterilized in a solution of 0.2% HgCl + 60 mM HCl for 3 min, imbibed for 8 h in distilled water, and germinated on wet paper towels until the radicle was 10–15 mm long. Seedlings were planted in sterilized sand and inoculated with either a pure culture of *Rhizobium phaseoli* strain CIAT 73 (an effective strain) or with 14c (an ineffective strain, isolated from *P. coccineus* by Dr. DONALD MUNNS). Plants were maintained on a nitrogen-free nutrient solution at 25 C for a 16-h day with a 20 C night temperature in a growth chamber. Light was supplied at 550 $\mu E\ m^{-1}\ s^{-2}$ from a mixture of fluorescent and incandescent sources.

At 3-day intervals after inoculation, root segments and nodules were collected for light (LM) and electron microscopy (EM). For LM observation of infection threads, segments from the root hair zone were fixed for 12 h in Carnoy's solution (6:3:1), rinsed in 70% ethanol, and stained for 3–5 s in .05% toluidine blue (PHILLIPS 1971). Nodule

Manuscript received September 1981; revised manuscript received October 1981.

Address for correspondence and reprints: LISA MORRISON BAIRD, Department of Agronomy and Range Science, University of California, Davis, California 95616.

samples for LM were fixed and processed according to standard procedures (BROOKS, BRADLEY, and ANDERSON 1950).

For EM observation, nodules were sliced to facilitate penetration of the fixative, 3% glutaraldehyde in a 0.1 M cacodylate buffer, pH 7.2. After 12-h fixation at room temperature, segments were postfixed in 2% OsO_4 in the same buffer for 2 h, rinsed, and slowly dehydrated through a graded ethanol series. Infiltration into SPURR's (1969) epoxy resin was carried out over a 2-day period. Tissues were then transferred to fresh resin in flat embedding molds and allowed to infiltrate under vacuum for 24 h prior to polymerization in a vacuum oven at 60 C for 24 h. Sections were cut at 600–900 Å on a diamond knife in an LKB IV ultramicrotome, mounted on uncoated copper grids, and stained in a saturated uranyl acetate solution for 30 min, followed by 30 min in lead citrate (REYNOLDS 1963). Specimens were examined in a JEOL 100S electron microscope at 80 kV.

For increased resolution in LM observations, some nodules fixed for EM were dehydrated to 95% ethanol and embedded in JB-4 plastic (Polysciences). Semithin sections (1–2 μm) were made with a glass knife in an ultramicrotome and stained with toluidine blue.

At weekly intervals plants were harvested for determination of dry weight and apparent N_2 fixation. Dry weight of plant parts was measured after 72 h at 70 C. Apparent N_2 fixation was determined on intact root systems of harvested plants, using the C_2H_4 reduction assay (HARDY et al. 1968).

Results

EFFECTIVE NODULATION

INFECTION PROCESS.—The first microscopic evidence of root nodule initiation in *Phaseolus vulgaris* inoculated with CIAT 73 is the presence of infection threads in root hairs 6–9 days after inoculation (figs. 1, 2). Infected hairs are frequently straight or only slightly curved at the tip; when stained with toluidine blue, the hair is blue to purple while the infection thread is brilliant red. The thread contains a tightly packed column of bacteria, and the apex of the thread is usually closely associated with the root hair nucleus. Although threads may branch after entering the root cortex, multiple infection threads were not observed within a single root hair. Within the cortex, infection threads grow both intra- and intercellularly to invade five to eight layers of cells. As the threads elongate between adjacent cells, host cell walls and plasmalemmae invaginate, giving rise to intracellular infection threads. Intracellular infection threads frequently distort the thin host cell wall, creating a funnel-shaped thread-wall junction. Threads often curve or branch within a cell, passing near but not through the nucleus, and semithin sections of incipient nodules reveal portions of the thread scattered

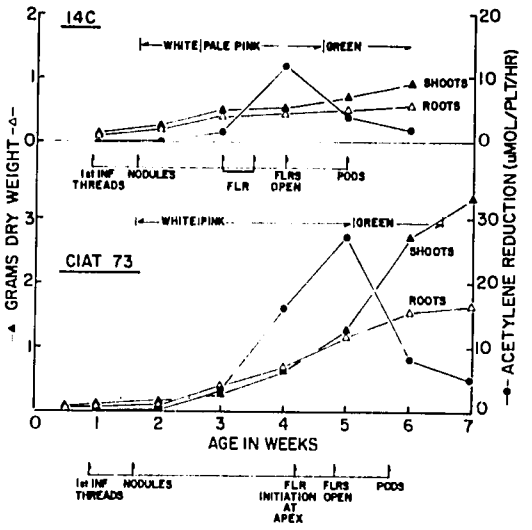

FIG. 1.—Comparative plant and nodule development following infection with the CIAT 73 or 14c strain of *Rhizobium phaseoli*. Note differences in nodule maturation and nitrogenase (acetylene reduction) activity as they correspond to dry-weight accumulation in roots and shoots and the time of floral initiation.

through the cytoplasm (fig. 3). In LM and EM cross sections, rod-shaped bacteria of the thread appear embedded in a matrix bounded by a cell wall and plasma membrane which are continuous with those of the host cell (figs. 3–5). Segments of rough endoplasmic reticulum (RER) and mitochondria are frequently observed in close association with developing intracellular threads (figs. 4–6).

Bacteria and portions of the thread matrix are released from the infection thread at unwalled regions at or close to the thread tip (fig. 4). This bacteria-matrix complex remains surrounded by host plasma membrane and forms an unwalled droplet. Invagination and "pinching off" of the plasma membrane ultimately release bacteria from the droplet.

NODULE DEVELOPMENT.—Bacterial release into cortical cells stimulates cell divisions, and infected cells stain densely (fig. 7). Divisions initially occur randomly and subsequently become localized in a broad band of cells which forms the nodule apex. Cell divisions and differentiation of procambial cells near the stele of the root give rise to vascular tissue which supplies the developing nodule. Proliferation of cortical parenchyma cells between the stele and the infected cortical area results in protrusion of a nodule on the root surface. In *P. vulgaris*, small white nodule protrusions are first evident 9–12 days after inoculation (fig. 1).

Two to 3 wk following inoculation, plants are in the second to third plastochron. Nodules are pale to rosy pink and 1–2 mm in diameter. Bacteria within cortical cells continue to increase by fission until most of the cytoplasm is occupied by the endophyte (fig. 8), and the cortical cells increase in size. Increase in the cellular area occupied by the endo-

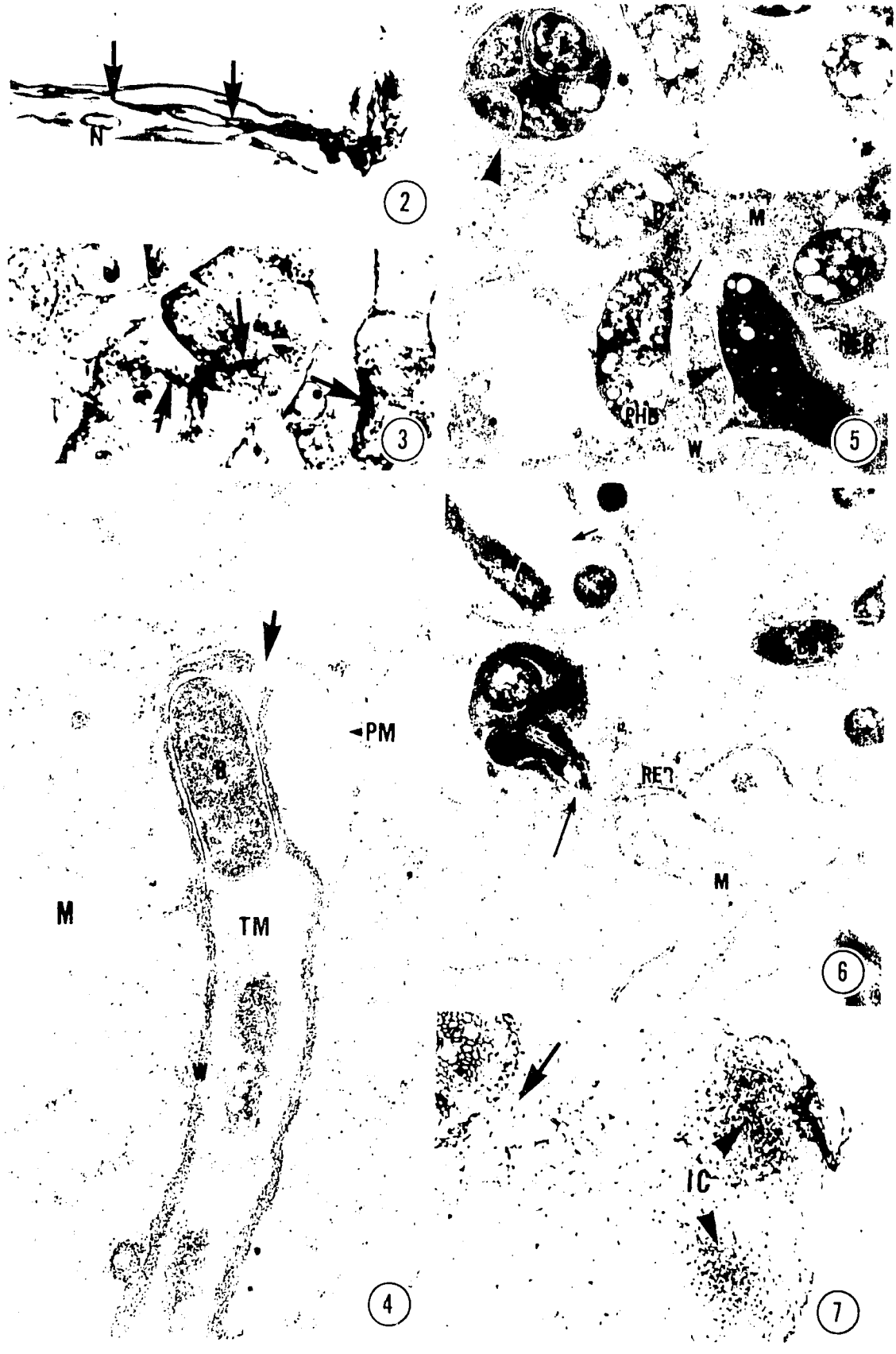

FIGS. 2–7.—LM and EM views of infectivity and effective early nodule development in *Phaseolus vulgaris*. Fig. 2, Whole root hair stained with toluidine blue to show infection thread (arrows) traversing the hair and closely associated with the hair nucleus. Note curvature of hair tip; × 2,400. Fig. 3, Semithin (1–2 μm) section of newly infected root cortical cells showing infection threads extending both intra- and intercellularly (arrows); × 3,500. Fig. 4, Intracellular infection thread comprised of bacteria and matrix, bounded by cell wall material, here discontinuous at the thread tip (arrow) and plasma membrane of the infected cell. Note numerous mitochondria close to infection thread; × 26,000. Fig. 5, Infection threads invading and within (arrowheads) cortical cell and released bacteria containing poly-β-hydroxybutyrate, surrounded by a membrane envelope (small arrow). Note mitochondrion and segments of RER near infection thread. Fig. 6, Characteristic organelles of the cytoplasm of infected cells, including long, slender profiles of RER, mitochondria, and newly released bacteria surrounded by a membrane envelope (arrows); × 13,000. Fig. 7, Early nodule development and protrusion, showing densely stained infected cells (arrowheads) and initial stages of procambial development adjacent to the stele (arrow); × 1,100. *B* = bacterium, *IC* = infected cells, *M* = mitochondrion, *N* = nucleus, *PHB* = poly-β-hydroxybutyrate, *PM* = plasma membrane, *RER* = rough endoplasmic reticulum, *TM* = thread matrix, *W* = cell wall.

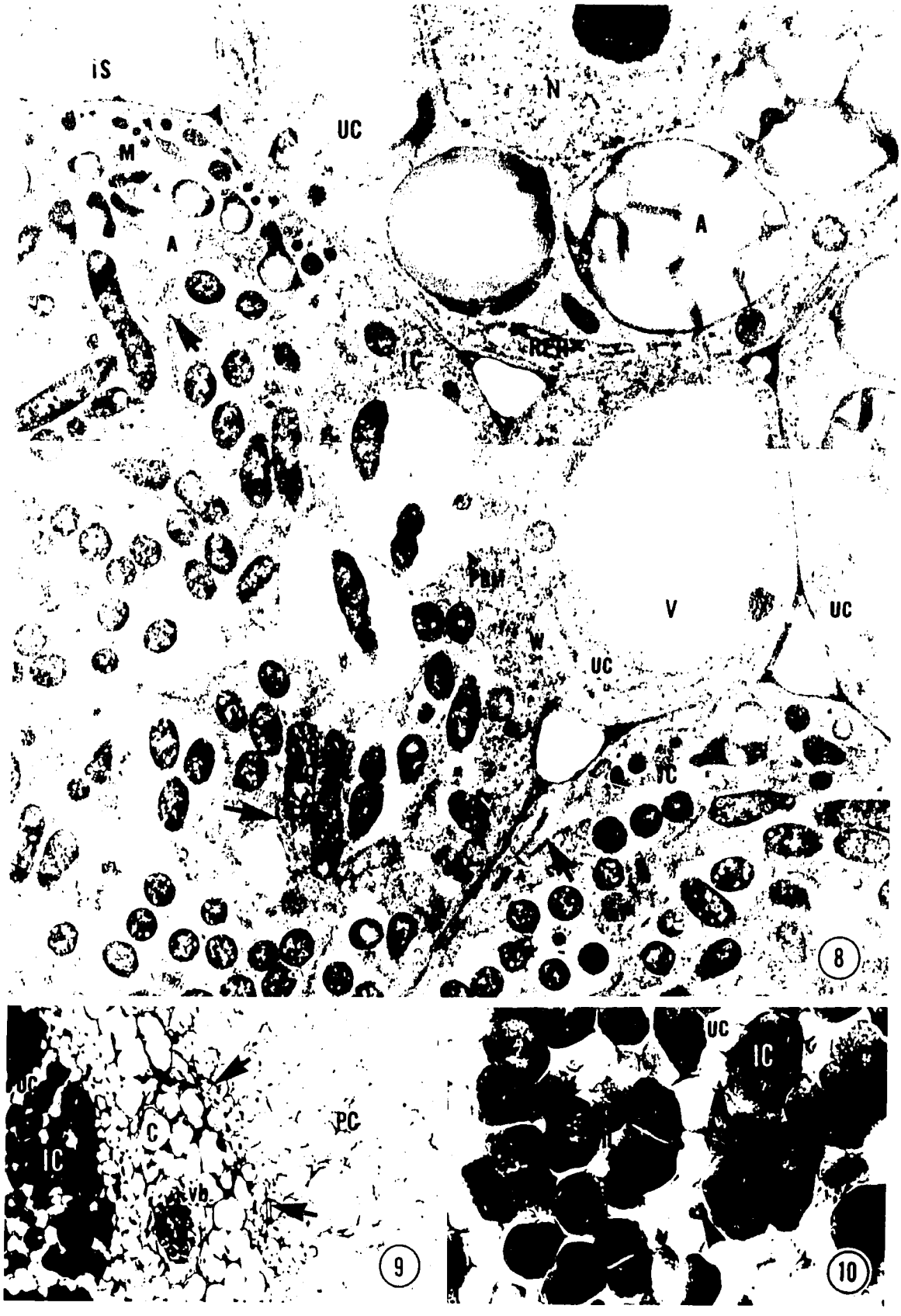

FIGS. 8–10.—LM and EM views of effective nodule maturation in *Phaseolus vulgaris*. Fig. 8, Montage of infected cells (left and lower right) and adjacent uninfected cells. Note numerous bacteroids within peribacteroid membranes interspersed with long segments of RER (arrows). Amyloplasts and mitochondria are confined to margins of the cytoplasm. In adjacent uninfected cells note large amyloplasts, broader conspicuous strands of RER, and mitochondria; × 10,000. Fig. 9, Mature nodule comprised of a core of large, densely stained infected cells interspersed with smaller, faintly stained uninfected cells; cortical cells, traversed by vascular tissue and bounded by an endodermis (arrows); and an outer region comprised of large, loosely packed parenchyma cells; × 2,000. Fig. 10, Large, densely stained infected nodule cells characterized by prominent central nuclei and nucleoli and smaller, faintly stained uninfected cells with peripheral nuclei (arrowheads); × 4,000. *A* = amyloplast, *Bd* = bacteroid, *C* = nodule cortex, *IC* = infected cell, *IS* = intercellular space, *M* = mitochondrion, *N* = nucleus, *n* = nucleolus, *PBM* = peribacteroid membrane, *PC* = parenchyma cells, *RER* = rough endoplasmic reticulum, *UC* = uninfected cell, *V* = vacuole, *vb* = vascular bundle, *W* = cell wall.

phyte confines most host cell organelles to the peripheral cytoplasmic regions of the cell, although short segments of RER remain scattered through the cytoplasm. Two to seven rhizobia are usually grouped within a peribacteroid membrane. A lipid-like storage product, poly-β-hydroxybutyrate, accumulates within the bacteria.

Adjacent uninfected cortical cells are smaller and more vacuolate than infected cells (fig. 8). They characteristically have long strands of RER paralleling the cell wall adjacent to an infected cell, and plasmodesmata are abundant in these wall regions. The most striking feature of uninfected cells, however, are the large ovoid amyloplasts which virtually fill the cytoplasm.

NODULE MATURITY.—Nodules reach structural and functional maturity 3–5 wk after inoculation. Acetylene reduction can first be measured 3 wk after inoculation; the rate increases rapidly, reaching a maximum at 5 wk (fig. 1). Nodules are 2–3 mm in diameter and deep pink with protruding ridges of white callus-like cells which are actually loosely packed parenchyma. Subtending the parenchyma is a single layer of endodermal cells. Small rectangular crystals, termed styloids by FRAZER (1942), are abundant in adjacent cells. Vascular tissue and parenchyma cells comprise the nodule cortex. Each vascular bundle is comprised of a central core of xylem surrounded by phloem and bounded by an endodermis. No transfer cells are observed in these bundles, but several densely cytoplasmic cells are present between the xylem and phloem. Parenchyma cells of the nodule cortex are filled with starch as long as the nodule is viable; remobilization of starch begins with nodule senescence.

The central portion of the nodule is comprised of both infected and uninfected cells. The bacteroid-filled, densely stained infected cells are large and round with small or no vacuoles, a centrally located prominent nucleus, and a darkly stained nucleolus (figs. 9, 10). The uninfected cells are small and rectangular with peripherally located nuclei, a single large vacuole, and several large oval amyloplasts.

Mature infected cells are filled with membrane-bound, rod-shaped bacteroids (fig. 11) which contain

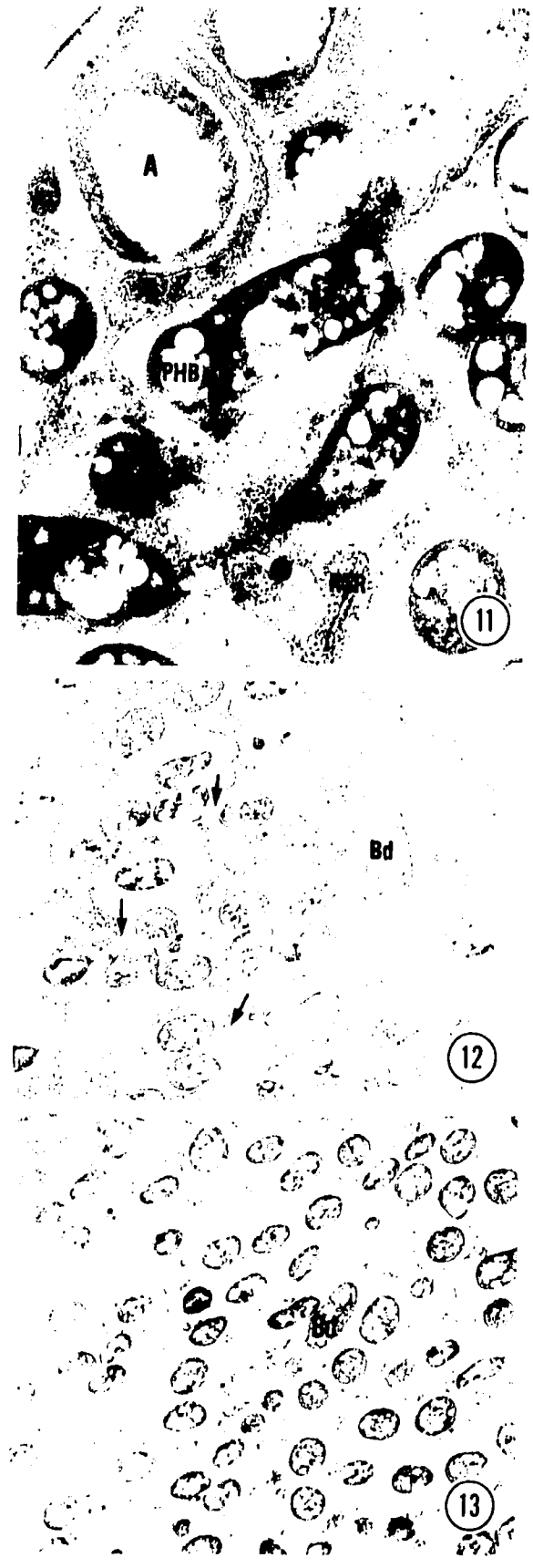

FIGS. 11–13.—EM views of effective mature and senescing nodules of *Phaseolus vulgaris*. Fig. 11, Mature nodule cell containing bacteroids with abundant depositions of poly-β-hydroxybutyrate, elongate mitochondrion cupped around amyloplast, and conspicuous short segments of RER; × 21,000. Fig. 12, Early nodule senescence, typified by localized disruptions of the peribacteroid membrane (arrows) and flocculent appearance of the cytoplasm; × 13,000. Fig. 13, Late nodule senescence, typified by disappearance of peribacteroid membrane and breakdown of cytoplasm. Note persistence of bacteroids; × 9,000. *A* = amyloplast, *Bd* = bacteroid, *M* = mitochondrion, *PHB* = poly-β-hydroxybutyrate, *RER* = rough endoplasmic reticulum.

large amounts of poly-β-hydroxybutyrate. The host cell cytoplasm is dense and contains few strands of RER. Near the periphery of the cell elongated mitochondria form close, cuplike associations with amyloplasts (fig. 11).

NODULE SENESCENCE.—The mature, functional nodule is relatively short lived. Between 5–6 wk after inoculation, acetylene reduction declines sharply (fig. 1), and nodules begin to turn green. Host cells become increasingly vacuolate, nuclei become lobed, and the cytoplasm begins to degenerate (figs. 12, 13). After a general increase in electron opacity, the cytoplasm appears flocculent. Mitochondria and plastids degenerate, and the peribacteroid membranes rupture. However, bacteria do not appear to undergo any significant ultrastructural changes until a large region of the nodule senesces.

INEFFECTIVE NODULATION

INFECTION PROCESS.—Infectivity with the ineffective strain of *Rhizobium phaseoli* (14c) occurs in a manner similar to that observed with the effective strain (CIAT 73); i.e., the infection thread penetrates and elongates through a root hair (fig. 14), branches extensively within the root cortex, and grows both inter- and intracellularly (fig. 15). Invaginations of the host cell wall give rise to intracellular infection threads from which membrane-bound droplets of thread matrix and bacteria are ultimately released into the host cytoplasm by invagination and "pinching off" of the surrounding host cell membranes. Bacteria vary in electron opacity and are frequently irregularly shaped (fig. 16). In most, a network of DNA fibrils of the nucleoid is visible, and occasionally electron-lucent areas develop within the bacteria. Some newly released bacteria are enclosed by an intact membrane (fig. 17); around other bacteria the membrane is partially disrupted (fig. 17).

Long and short strands of RER are scattered throughout the cytoplasm of newly infected cells, often lying close to infection threads and unwalled droplets (fig. 16); some segments of RER appear swollen or separated (figs. 16, 17). Mitochondria are numerous and often closely associated with unwalled droplets (fig. 16). Golgi bodies are conspicuous, and numerous vesicles are scattered throughout the cytoplasm. Plastids are small and contain small depositions of starch. The nucleus is approximately three times larger than that of adjacent uninfected cells and tends to be lobed with a prominent nucleolus. Cytoplasmic vacuolation is minimal.

NODULE DEVELOPMENT AND MATURITY.—Four weeks after inoculation, ineffectively nodulated plants are chlorotic and about one-half the height of effectively nodulated plants; the leaf area of these plants is similarly reduced. The maximum rate of acetylene reduction occurred at 4 wk (fig. 1). Most ineffectively nodulated plants also make the transition to flowering at 4 wk. The oldest nodules are pale pink, and their cellular organization is similar to that of effective nodules. Cells of ineffective nodules, however, typically show vacuolated infected cells and lobed nuclei.

Ultrastructurally, the cytoplasm of infected cells in an ineffective nodule is nearly electron lucent. There are few free ribosomes, but many strands of partially dilated RER are evident. Golgi bodies are prominent, and small vesicles are scattered through the cytoplasm. Numerous mitochondria and starch-free plastids are clustered near the cell walls and intercellular spaces.

Bacteroids are scattered throughout the cytoplasm, but they are less numerous and lack the large accumulation of poly-β-hydroxybutyrate observed in effective nodules. Bacteroids are frequently bound by partial membrane envelopes which often have associated numerous membrane fragments and vesicles (fig. 18). Segments of RER are often in close proximity to the membrane envelopes (figs. 18, 19). Occasionally bacteria appear to be released into cytoplasmic vacuoles (fig. 19). This process involves invagination of the tonoplast and liberation of three to five free bacteria and membrane fragments within the vacuole.

Uninfected cortical cells surround the central core of the nodule and are numerous within the central bacteroid zone; short, stacked segments of RER frequently parallel cell walls adjacent to walls of infected cells. Few mitochondria and Golgi bodies are present in uninfected cells. Such cells characteristically have a small nucleus usually confined to the periphery of the cell, a large central vacuole, and several amyloplasts which contain large ovoid starch grains (fig. 18).

NODULE SENESCENCE.—Between the fourth and fifth week after inoculation, cells within the nodule begin to degenerate (figs. 20–23). The cytoplasm becomes electron lucent with a few short strands of RER and Golgi bodies and degenerating mitochondria and plastids. Membrane envelopes surrounding the bacteria are ruptured, and membrane fragments and vesicles are abundant. Most bacteria appear ultrastructurally unchanged during these initial stages of nodule breakdown.

Discussion

Numerous studies document the development of effective root nodules in peas (BOND 1948; NEWCOMB 1976), soybeans (BIEBERDORF 1938; GOODCHILD and BERGERSEN 1966; WERNER and MÖRSCHEL 1978), and alfalfa (JORDAN, GRINYER, and COULTER 1963; BASSETT et al. 1977*a*, 1977*b*). In some respects, effective nodule development in *Phaseolus vulgaris* resembles that in these better-researched genera. In *P. vulgaris*, newly released bacteria contain little

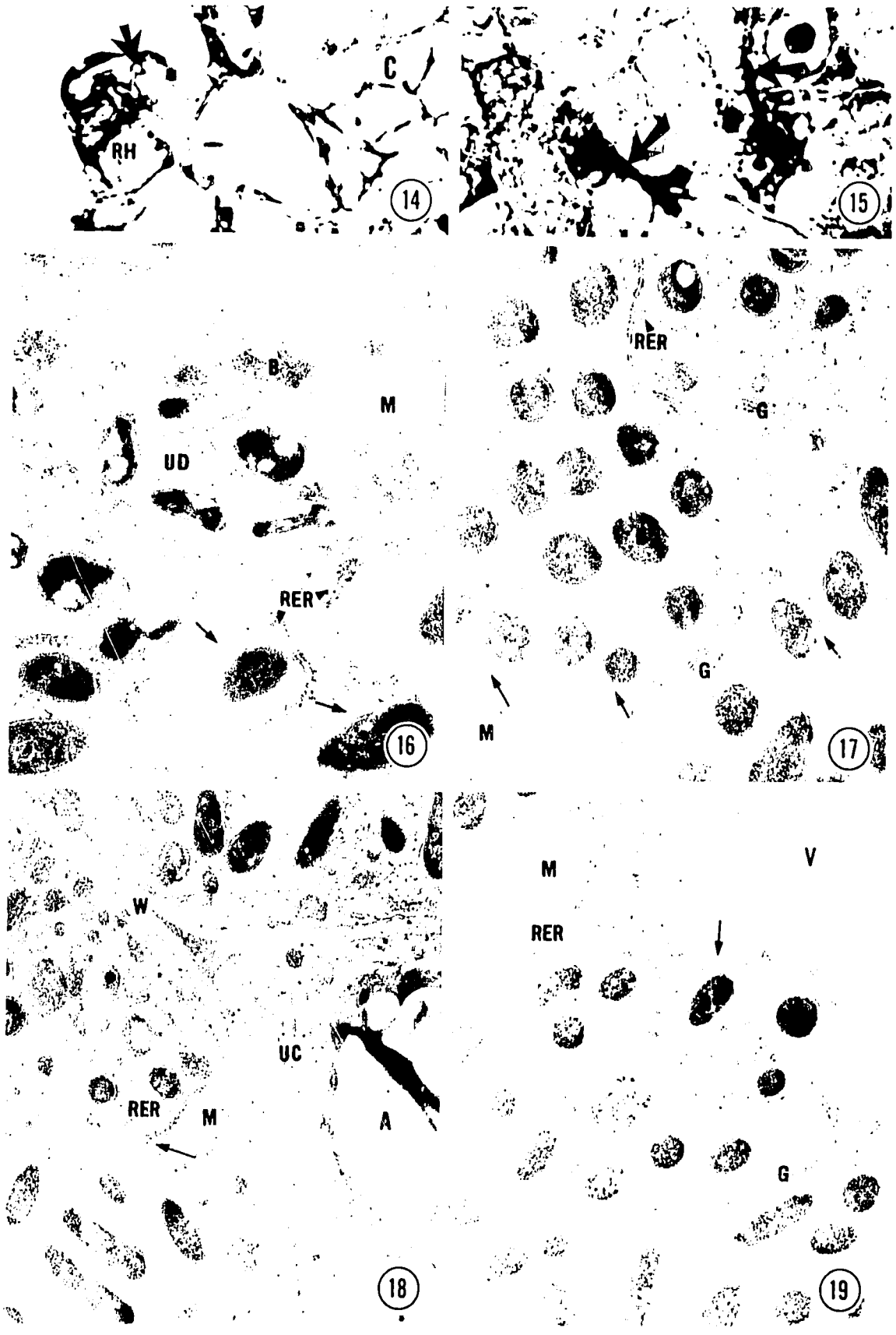

FIGS. 14-19.—LM and EM views of infectivity and ineffective nodule development in *Phaseolus vulgaris*. Fig. 14, Whole root hair stained with toluidine blue to show infection thread (arrow) in curved root hair; × 4,000. Fig. 15, Semithin (1-2 μm) section of newly infected root cortical cells with extensively branched infection thread (arrows) growing inter- and intracellularly; × 4,600. Fig. 16, Unwalled droplet within host cytoplasm of newly infected cortical cell. Note irregular shapes of bacteria within the unwalled droplet, the apparent partial disruption of the membrane surrounding released bacteria (arrows) and proximity to droplets of mitochondria and RER; × 16,000. Fig. 17, Typical infected host cell cytoplasm filled with bacteria surrounded by a tenuous or locally discontinuous membrane (arrows). Note numerous Golgi bodies, mitochondria, and RER; × 15,000. Fig. 18, Infected cells (left and above) and adjacent uninfected cell 3 wk after inoculation. Note plastids and mitochondria clustered near walls, strands of RER in infected cells, and large ovate amyloplast typical of uninfected cells; × 12,000. Fig. 19, Apparent release of bacteria into vacuole of host cell, 3 wk after inoculation. Note characteristic host cell organelles, including Golgi, RER, and mitochondria; × 8,500. *A* = amyloplast, *B* = bacterium, *C* = cortex, *G* = Golgi apparatus, *M* = mitochondrion, *P* = plastid, *RER* = rough endoplasmic reticulum, *RH* = root hair, *UC* = uninfected cell, *UD* = unwalled droplet, *V* = vacuole, *W* = cell wall.

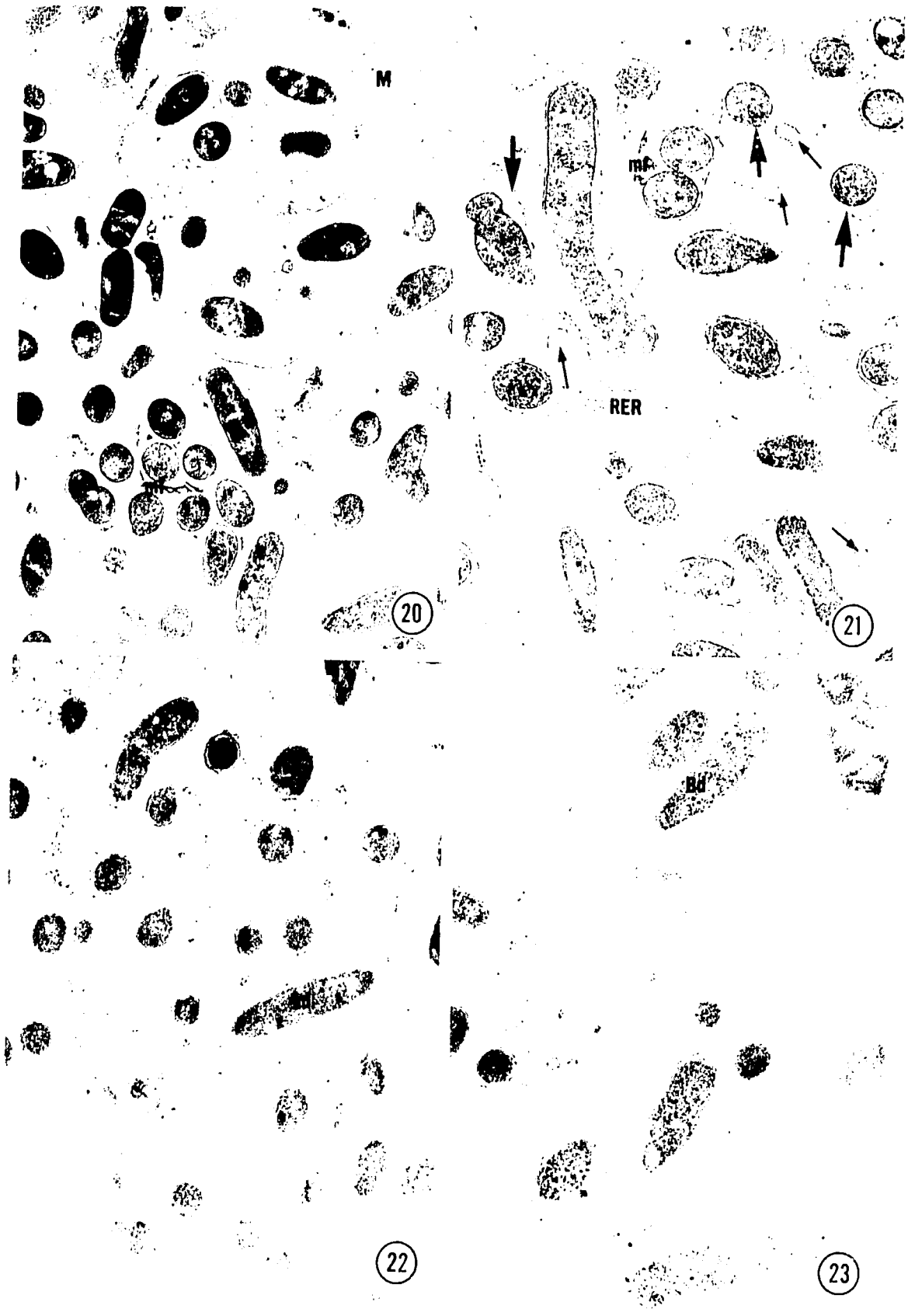

FIGS. 20-23.—EM views of mature and senescing cells of ineffective nodules. Fig. 20, Bacteroids after 4 wk, enclosed in tenuous membranes which are frequently disrupted. Cytoplasm appears nearly translucent, with mitochondria and plastids clustered near the cell wall; × 11,000. Fig. 21, 96 h after fig. 20, showing strands of RER and vesicles (small arrows) scattered through the thin cytoplasm. Note numerous discontinuities of peribacteroid membrane (large arrows); × 13,000. Fig. 22, Senescent nodule cell with bacteria still intact in a thin, vesicle-filled cytoplasm; × 11,000. Fig. 23, Same stage as fig. 22, showing disrupted membranes of bacteria and membrane fragments and vesicles scattered through the electron-lucent cytoplasm; × 14,000. *Bd* = bacteroid, *M* = mitochondrion, *mf* = membrane fragment, *P* = plastid, *RER* = rough endoplasmic reticulum.

storage product, and release of bacteria is accompanied by a transitory increase in host cell RER, mitochondria, and Golgi bodies. These characteristics have been noted frequently in other legumes (DART and MERCER 1964; GOODCHILD and BERGERSEN 1966; NEWCOMB 1976). Although plastids in infected cells of *P. vulgaris* accumulate more starch as nodule development progresses, the number and size of the infected cell amyloplasts contrast sharply with the large, rectangular deposits of starch in infected pea cells (NEWCOMB 1976) and with the large ovoid amyloplasts in soybean (WERNER and MÖRSCHEL 1978). Most starch storage in *P. vulgaris* nodules occurs in uninfected cells of the bacteroid zone and in cortical cells.

In *P. vulgaris*, probably the most remarkable structural change in host cell organelles during effective nodulation occurs in mitochondria. These become extremely elongated and closely associated with starch-filled plastids near the periphery of the cell. The elongation and plastid–mitochondrial associations are first observed 16 days after inoculation and are most conspicuous between 3–5 wk. As plant cells increase in volume, bacteria multiply and become bacteroidal, and ultimately, peak nitrogen fixation (as indicated by acetylene reduction activity) is reached. All of these activities require a high energy turnover, which is perhaps facilitated by apposition of mitochondria and plastids.

Similar associations of mitochondria and plastids were observed in soybean nodules by WERNER and MÖRSCHEL (1978), who suggested, on the basis of correlation of electron microscopic data with measurement of nitrogenase activity, that this association could be considered a cytological marker for peak nitrogen fixation. They likened the elongated mitochondrion and its expanded cristae to those observed in cardiac muscle (FAWCETT 1966), in which high energy turnover is a necessity.

Elongated, dumbbell-shaped mitochondria such as those observed in *Phaseolus* and *Glycine* nodules have also been noted in cells of other metabolically active tissue (STEMPAK 1967; BAGSHAW, BROWN, and YEOMAN 1969). On the basis of serial sections, STEMPAK (1967) proposed a three-dimensional cup-shaped model for the bell-shaped mitochondrial profiles and suggested that they might represent stages in mitochondrial division. While the cup-shaped mitochondrion-amyloplast complex in nodules could represent an efficient high-energy conformation, it is also conceivable that this configuration is a prelude to mitochondrial fission and/or a mechanism to increase the surface area of mitochondrial membranes in response to a high energy requirement.

Comparison of morphogenesis of effectively and ineffectively nodulated plants suggests that ineffective nodulation may accelerate the process of normal nodule senescence in *P. vulgaris*. Infection with the 14c strain of *Rhizobium phaseoli* and early nodule development resemble in many respects the initial stages of development of an effective nodule. Some bacteria appear irregularly shaped at the time of release from the infection thread and are surrounded by a complete or nearly complete membrane envelope. The presence and integrity of this membrane have been considered critical in the establishment of nitrogen fixation in the nodule (KIJNE 1975; VERMA, HUNTER, and BAL 1978). As nodule development continues in *P. vulgaris*, membrane fragments or vesicles are observed adjacent and adhering to the membrane envelope, which frequently becomes discontinuous or disrupted. Disruption is often observed in very old, effective nodule cells of peas and has been associated with nodule senescence (TRUCHET and COULOMB 1973; KIJNE 1975).

In host cells of ineffective nodules of *P. vulgaris*, the accumulation of RER and the profiles of Golgi apparatus are conspicuous throughout nodule development. This contrasts strikingly with effective nodules in *P. vulgaris* and other species in which only short segments of RER and a minimal number of Golgi bodies are noted once the nodule attains maturity (MACKENZIE and JORDAN 1974; WERNER and MÖRSCHEL 1978). Numerous mitochondria are present in cells of ineffective *Phaseolus* nodules, both in association with unwalled droplets and along cell walls and intercellular spaces; however, the elongated mitochondrion–amyloplast complex in effective nodules of *Phaseolus* and soybean (WERNER and MÖRSCHEL 1978) has not been observed in ineffective nodules. Extensive RER development and numerous mitochondria have been associated with ineffective nodule development in alfalfa (MACKENZIE and JORDAN 1974) and have been related to host cell response to nitrogen starvation.

By the time nitrogen fixation is measured in ineffectively nodulated *P. vulgaris* plants, the shoots are chlorotic, lower leaves have abscised, and under nitrogen stress, the plant has made the transition to flowering. The onset of flowering in ineffectively nodulated plants coincides with the beginning of rapid nodule degeneration. This degenerative process is similar to that in effectively nodulated plants and does not appear to involve rejection or selective autolysis of the bacteria, as in soybeans (BASSETT et al. 1977*b*) and alfalfa (MACKENZIE and JORDAN 1974).

From our observations, we speculate that carbohydrate and/or nitrogen partitioning may be the basis of the lack of coordination between the plant and bacterium in ineffective symbiosis. The importance of such partitioning in a symbiotic relationship is supported by studies suggesting that size and longevity of nodules in ineffective symbioses is related to carbohydrate deficiency due to stunted plant growth (JORDAN and GARRARD 1951). JORDAN and GARRARD attributed cytological disruption in

such ineffective nodule cells to bacterial attack on the host cell. Subsequent work on alfalfa (MacKenzie and Jordan 1974) indicated that ineffective nodulation was only an acceleration to a greater or lesser degree of the degenerative processes which occur in an effectively nodulated plant. MacKenzie and Jordan considered the presence of ineffective bacteria less important than the evidence of nitrogen starvation in the host cell, and they stated that normal breakdown of nodule tissue in effectively nodulated plants might also be the result of nitrogen starvation resulting from the demand for nitrogen during pod filling.

Recent work on the translocation of ^{14}C photosynthate during reproductive development in *P. vulgaris* (Waters et al. 1980) suggests that leaves at the lower nodes are primarily responsible for carbohydrate supply to the nodule. Yellowing or abscission of these leaves results in reduction of the photosynthate supply to the nodule. In our study, the chlorosis of lower leaves, coupled with the early transition to flowering, could have severely restricted carbohydrate and nitrogen in the nodule and, therefore, accelerated the process of senescence. Research is currently in progress to investigate both carbohydrate and nitrogen partitioning in effectively and ineffectively nodulated plants to determine the relative contributions of each to the maintenance of nodule integrity.

Acknowledgments

This investigation represents a portion of a thesis submitted by Lisa Morrison Baird in partial fulfillment of the requirements for the Ph.D. degree at the University of California, Davis. We acknowledge with gratitude support of USDA subgrant 701-15-19, PASA 610-9-76, financed by the Agency for International Development to B. D. Webster, and Jastro Shields research scholarships and a Sigma Xi Grant-in-Aid of Research to L. M. Baird.

LITERATURE CITED

Bagshaw, V., R. Brown, and M. M. Yeoman. 1969. Changes in the mitochondrial complex accompanying callus growth. Ann. Bot. **33**:35-44.

Bassett, B., R. N. Goodman, and A. Novacky. 1977*a*. Ultrastructure of soybean nodules. I. Release of rhizobia from the infection thread. Can. J. Microbiol. **23**:573-582.

———. 1977*b*. Ultrastructure of soybean nodules. II. Deterioration of the symbiosis in ineffective nodules. Can. J. Microbiol. **23**:873-883.

Bergersen, F. J. 1957. The structure of ineffective nodules of legumes: an unusual type of ineffectiveness and an appraisal of present knowledge. Australian J. Biol. Sci. **10**:233-242.

———. 1974. Formation and function of bacteroids. Pages 473-498 *in* A. Quispel, ed. The biology of nitrogen fixation. North Holland, Amsterdam.

Bieberdorf, F. W. 1938. The cytology and histology of the root nodules of some Leguminosae. J. Amer. Soc. Agron. **30**:375-389.

Bond, L. 1948. Origin and developmental morphology of root nodules of *Pisum sativum*. Bot. Gaz. **109**:411-434.

Brooks, R. M., M. V. Bradley, and T. I. Anderson. 1950. Plant microtechnique manual. University of California, Davis.

Chen, H. K., and H. G. Thornton. 1940. The structure of "ineffective nodules" and its influence on nitrogen fixation. Proc. Roy. Soc. London **129**:208-229.

Dart, P. J., and F. V. Mercer. 1964. Fine structure changes in the development of the nodules of *Trifolium subterraneum* L. and *Medicago tribuloides* Desr. Arch. Microbiol. **49**:209-235.

Dawson, M. 1900. Nitragin and the nodules of leguminous plants. Phil. Trans. Roy. Soc. London **192**:1-28.

Fawcett, D. W. 1966. An atlas of fine structure, the cell, its organelles and inclusions. Saunders, Philadelphia, London.

Frank, B. 1890. Ueber die Pilzsymbiose der Leguminosen. Landwirt. Jahrb. **19**:523-640.

Frazer, H. L. 1942. The occurrence of endodermis in leguminous root nodules and its effect upon nodule function. Proc. Roy. Soc. Edinburgh **61**:328-343.

Fred, E. B., I. L. Baldwin, and E. McCoy. 1932. Root nodule bacteria and leguminous plants. Univ. Wisconsin Stud. Sci. 5.

Goodchild, D. J., and F. J. Bergersen. 1966. Electron microscopy of the infection and subsequent development of soybean nodule cells. J. Bacteriol. **92**:204-213.

Graham, P. H., and J. Halliday. 1977. Inoculation and nitrogen fixation in the genus *Phaseolus*. Pages 313-334 *in* J. M. Vincent, A. S. Whitney, and J. Bose, eds. Exploiting the legume-rhizobium symbiosis in tropical agriculture. Univ. Hawaii College Trop. Agr. Misc. Pub. 145.

Hardy, R. W. F., R. P. Holsten, E. K. Jackson, and R. C. Burns. 1968. The acetylene-ethylene assay for nitrogen fixation: laboratory and field evaluation. Plant Physiol. **43**:1185-1207.

Holl, F. B. 1973. A nodulating strain of *Pisum* unable to fix nitrogen. Plant Physiol. **51**(suppl.):35.

Jordan, D. C., and E. H. Garrard. 1951. Studies on the legume root nodule bacteria. I. Detection of effective and ineffective strains. Can. J. Bot. **29**:360-372.

Jordan, D. C., I. Grinyer, and W. H. Coulter. 1963. Electron microscopy of infection threads and bacteria in young root nodules of *Medicago sativa*. J. Bacteriol. **86**: 125-137.

Kijne, J. W. 1975. The fine structure of pea root nodules. 2. Senescence and disintegration of the bacteroid tissue. Physiol. Plant Pathol. **7**:17-21.

Lima Nogueira, N. de, D. Martins da Silva, and S. M. T. Saito. 1979. Estudo ao microscopio electronico de nodulos em *Phaseolus vulgaris* L. causados por uma estirpe inefetiva de *Rhizobium*. Turrialba **29**:93-96.

McCoy, E. F. 1929. A cytological and histological study of the root nodules of the bean, *Phaseolus vulgaris* (L.). Zentrabl. Bakteriol. Abt. 2, **79**:394-412.

MacKenzie, C. R., and D. C. Jordan. 1974. Ultrastructure of root nodules formed by ineffective strains of *Rhizobium meliloti*. Can. J. Microbiol. **20**:755-758.

Newcomb, W. 1976. A correlated light and electron microscopic study of symbiotic growth and differentiation in *Pisum sativum* root nodules. Can. J. Bot. **54**:2163-2186.

Newcomb, W., K. Syōno, and J. G. Torrey. 1977. Development of an ineffective pea root nodule: morphogenesis, fine structure and cytokinin biosynthesis. Can. J. Bot. **55**: 1891-1907.

Pankhurst, C. E. 1974. Ineffective *Rhizobium trifolii* mutants examined by immuno-diffusion, gel-electrophoresis and electron-microscopy. J. Gen. Microbiol. **82**:405-413.

Phillips, D. A. 1971. Abscisic acid inhibition of root nodule

initiation in *Pisum sativum*. Planta **100**:181–190.

REYNOLDS, E. S. 1963. The use of lead citrate at high pH as an electron-opaque stain in electron microscopy. J. Cell Biol. **17**:108.

SCHNEIDER, A. 1892. Observations on some American Rhizobia. Bull. Torrey Bot. Club **19**:203–219.

SEARS, O. H., and F. M. CLARK. 1930. Non-reciprocal cross-inoculation of legume nodule bacteria. Soil Sci. **30**:237–242.

SPURR, A. R. 1969. A low-viscosity epoxy resin embedding medium for electron microscopy. J. Ultrastructure Res. **26**:31–43.

STEMPAK, J. 1967. Serial section analysis of mitochondrial form and membrane relationships in the neonatal rat liver cell. J. Ultrastructure Res. **18**:619–636.

TRUCHET, G., and P. COULOMB. 1973. Mise en évidence et évolution du système phytolysosomal dans les cellules des différentes zones de nodules radiculaires du Pois (*Pisum sativum* L.). Notion d'heterophagie. J. Ultrastructure Res. **43**:36–57.

VERMA, D. P. S., N. HUNTER, and A. K. BAL. 1978. Asymbiotic association of *Rhizobium* with pea epicotyls treated with plant hormone. Planta **138**:107–110.

WATERS, L., JR., P. J. BREEN, H. J. MACK, and P. H. GRAHAM. 1980. Translocation of ^{14}C-photosynthate, carbohydrate content, and nitrogen fixation in *Phaseolus vulgaris* L. during reproductive development. J. Amer. Soc. Hort. Sci. **105**:424–427.

WERNER, D., and E. MÖRSCHEL. 1978. Differentiation of nodules of *Glycine max*. Planta **141**:169–177.

WILSON, J. K., and E. W. LELAND. 1929. The value of supplementary bacteria for legumes. J. Amer. Soc. Agron. **2**:574–586.